RESEARCH ARTICLE

Macromolecular Materials and Engineering
Open Access
www.mame-journal.de

Adsorbable and Antimicrobial Amphiphilic Block Copolymers with Enhanced Biocompatibility

Cornelia Wolf-Brandstetter, Rafael Methling, and Dirk Kuckling**

To minimize or avoid the use of antibiotics, antimicrobial polymers have emerged as a promising option to fight biomaterial-associated infections, e.g., on titanium-based implants. However, the challenge is to develop active polymers that exhibit an antimicrobial effect and are compatible with human cells. Different studies aiming for biocidal polymers active in soluble mode, focused on the ratio of cationic to hydrophobic groups, while only marginal knowledge is available for immobilized components. Here a strong hydrophilic electrolyte 4-vinylbenzyltrimethylammonium chloride (TMA) is chosen as the cationic component. The block composition of the polycationic segment is modified with styrene (Sty) regarding the amphiphilic balance. To adsorb such polymers onto titanium surfaces they are equipped with a polyphosphonic acid anchor block by sequential reversible-addition-fragmentation chain-transfer polymerization (RAFT) polymerization. The polymer composition affected the wetting behavior of adsorbed coatings with water contact angles ranging from 17° to 72°, while zetapotential measurements confirmed high extent of positive charges for all adsorbed polymer coatings. The fundamentally modified block composition resulted in significantly improved cytocompatibility. Antimicrobial efficacy in early bacterial adhesion is still retained from slightly antiadhesive coatings to combined antiadhesive/biocidal activity depending on Sty/TMA ratio in random polymers while a block copolymer revealed lowest antimicrobial effect.

1. Introduction

Today's medical advances enable the restoration of damaged body functions through permanently implanted biomaterials. However, although materials and shape can vary greatly, all of them are prone to attract microorganisms and thus represent niches for infections in vivo.[1,2] Resulting infectious diseases are increasingly becoming a problem in the biomedical field. For a long time, an effective means of preventing and controlling microbial infections was the administration of antibiotics. However, the widespread and careless use of antibiotics has led to antibiotic-resistant microorganisms. In the worst cases, such biomaterial associated infections can lead to life-threatening situations but in any way result in increased costs in the health system.[3] In order to minimize or avoid the use of antibiotics, material scientists have turned to developing alternative methods to prevent microbial contamination. Antimicrobial polymers have emerged as a promising option as they provoke antimicrobial mechanisms that cannot be outwitted by pathogens and can be easily adapted to different applications.[4] The underlying mechanisms can be roughly divided into anti-adhesive (antifouling) or antimicrobial effects.[4] Among the various biocidal materials, cationic polymers based on quaternary ammonium have been shown to exhibit high efficacy. The mode of action is typically assigned to a damage of the outer and cytoplasmic membranes of bacteria, followed by bacterial cell lysis.[5,6] However, also human cell membranes might be adversely affected by a similar interaction.

As we have shown in a previous study, cationic polymer brushes with the general structure poly(1-propyl-4-vinylpyridinium bromide-block-4-vinylbenzylphosphonic acid) P(VPPr-b-VBPA) are easily applicable diblock copolymers that form polymer brushes via "grafting to" mechanism on titanium. The modified material is associated with good antimicrobial properties but insufficient cytocompatibility.[7] A potential way to control toxicity to human cells is copolymerization with monomers containing hydrophobic or uncharged hydrophilic groups aiming for an optimized amphiphilic balance. To this end, numerous studies have investigated the nature and ratio of cationic and hydrophobic groups with respect to their activity, with three main approaches i) the segregated approach with randomly distributed non-polar and cationic monomers, ii) the facially amphiphilic approach, with cationic and non-polar section in each repeat unit or iii) the "same centered" approach

C. Wolf-Brandstetter
Max Bergmann Center of Biomaterials
Technische Universität Dresden
Budapester Str. 27, 01069 Dresden, Germany
E-mail: cornelia.wolf-brandstetter@tu-dresden.de
R. Methling, D. Kuckling
Department of Chemistry
Paderborn University
Warburger Straße 100, 33098 Paderborn, Germany
E-mail: dirk.kuckling@uni-paderborn.de
The ORCID identification number(s) for the author(s) of this article can be found under https://doi.org/10.1002/mame.202500078

DOI: 10.1002/mame.202500078

with hydrophobic moieties directly attached to the cationic component.[8] The main method to vary the amphiphilic balance was to change the nature of the hydrophobic unit, mainly by changes in the alkyl length. However, only recently also the nature of the hydrophilic units was addressed.[9,10] It has to be highlighted that all these investigations refer to soluble polymers that change their 3D structure upon interaction with either bacterial or human cell membrane. In contrast, only marginal knowledge is available for immobilized components, particularly for polymers that are not grafted from surfaces but can be adsorbed to the surfaces of interest. Therefore, the idea of our study was to find a polymer composition that is adsorbable, not or less toxic to human cells but still antimicrobial. For this purpose, we exchanged the cationic component and started with an inherently cationic monomer, 4-vinylbenzyltrimethylammonium chloride (TMA), which also saved a post-processing step, while styrene (Sty) was used as the hydrophobic comonomer to adjust the amphiphilic balance. TMA is a strong electrolyte and its efficacy in antimicrobial applications has already been demonstrated in various studies.[11,12] Among the different potential options to adjust the hydrophobic/hydrophilic balance this strategy belongs to the so called "segregated monomer" approach,[8] where the feed ratio between the two monomers is varied to obtain the intended changes in polymer properties. In addition to this approach for obtaining random copolymers, a block copolymer was also synthesized in which the antimicrobial polycationic and the hydrophobic block are separated. Finally, titanium surfaces coated with these polymers were characterized in terms of their physicochemical properties, antimicrobial efficacy and by means of biocompatibility tests.

2. Results and Discussion

2.1. Tuning the Amphiphilic Balance

As in the previously published work, poly(dimethyl-4-vinylbenzylphosphonate) P(DMVBP) was used as an anchor block precursor.[7] Regarding the anchor block length, it was found that in the range from $n = 3$ to $n = 21$ a higher grafting density could be achieved by adsorption with increasing number of phosphonate groups. However, chains with 21 anchor groups were no longer water-soluble and are therefore less suitable for the application. Since comparable grafting densities were found for a block length between 11 and 16, an anchor block length of $n = 12$ was selected for the current study to ensure high surface affinity and good solubility in water.

TMA was synthesized by reacting 4-vinylbenzyl chloride with trimethyl amine in ethanol and purified by recrystallization from acetonitrile which afforded the product as hygroscopic, colorless crystals. The monomer proved compatible with the macro-RAFT agent P(DMVBP) derived from DMP when polymerized in dimethylformamide (DMF)/water mixtures with azobisisobutyronitrile (AIBN) as initiator at 70 °C. The monomer conversion was >90% and the polymer was isolated either by dialysis or precipitation in isopropanol. Although the molar mass of the polymer was over one magnitude higher than the molar mass cutoff of the membrane, a significant portion was lost during dialysis resulting in a yield of only 57%. Precipitation affords the product in a higher yield, however, DMF and isopropanol were not removed entirely.

The kinetics of the copolymerization of TMA and Sty with [TMA]:[Sty]:[P(DMVBP$_{12}$)]:[AIBN] = 100:90:1:0.2 were investigated. The reaction was performed with ≈0.6 M monomer concentration in DMF/water (3/2 v/v) at 70 °C. It must be noted that the removal of oxygen was conducted by three freeze-pump-thaw cycles, because it was observed that purging with argon removed significant amounts of the volatile Sty from the reaction mixture, leading to distorted results. While the samples for nuclear magnetic resonance (NMR) studies were retrieved according to the standard procedure (freezing under air and dilution in deuterated solvent), the size exclusion chromatography (SEC) samples had to be isolated via dialysis. It was observed that the removal of solvent in vacuo at 40 °C could cause free Sty to polymerize, resulting in bimodal distributions in SEC that were not representative. The first order kinetic plot for the total monomer concentration revealed a linear dependence up to a total conversion of 84% indicating the absence of termination reactions (**Figure 1A**). The reaction then reached a total conversion of 91% after 24 h with a slight drop in reaction rate. Although the reactive site is the same for both monomers, Sty was incorporated significantly faster than TMA (Figure 1B). It is known that the overall polarity can exert severe influence on the reaction rate in copolymerizations: the local concentration of a monomer at the active center depends on the preferential sorption of the polymer coil.[13,14] This affects the relative reactivity and leads to derivations from random incorporation of two competing species. Due to the pronounced difference in polarity of the monomers at hand, such a mechanism is also conceivable, although no further experiments were conducted to support this assumption.

The resulting structure exhibits a gradient composition of the second polymer block with a Sty-rich beginning and successively more TMA-units toward the end. At 25% total conversion, the block is nearly completely composed of Sty, whereas the overall composition after 24 h is close to the feed ratio. The final monomer conversion corresponds to the relative reactivities and amounts to 91% for Sty (degree of polymerization $P_n = 82$) and 73% for TMA ($P_n = 73$). The uneven incorporation also reflects in the average molar weights derived from SEC: an increase with a gradually steepening slope can be observed which can be explained with the higher molar mass of TMA compared to Sty (**Figure 2**). This is in good agreement with the theoretical values derived from NMR spectroscopy. The dispersity decreases at first, then increases after 40% total conversion and finally amounts to 1.51 which is slightly higher than expected for optimized RAFT polymerizations but satisfactory considering the chain extension with monomers of severely different polarities.

Based on the investigated system, five polymers with varying hydrophobicity were synthesized by chain extension of P(DMVBP$_{12}$) (**Figure 3** and **Table 1**) in order to screen the optimum between bactericidal effect and cell toxicity. The ratio of Sty to TMA in the final polymer was varied from zero to 2.04. The triblock copolymer AP5 was obtained by isolation of P(DMVBP$_{12}$-b-TMA$_{89}$) and subsequent chain extension with Sty followed by hydrolysis. It has been shown that a blocked structure as opposed to a random copolymer has an effect on selectivity in amphiphilic antimicrobial polymers.[15] In this way, the relative order of the polycationic and hydrophobic components has been reversed so

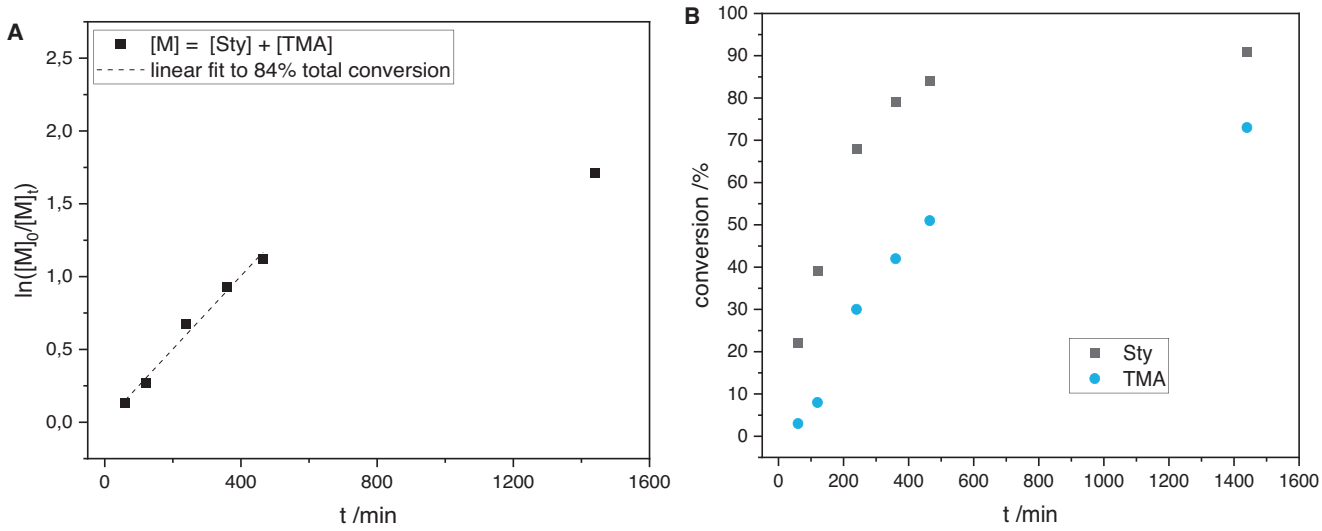

Figure 1. Kinetic investigations of [TMA]:[Sty]:[CTA]:[I] = 100:90:1:0.2 DMF/H_2O (1:1 v/v). A) Pseudo-first-order kinetic plot for total monomer conversion. B) Conversion determined via ^{1}H NMR sampling of Sty and TMA over time.

that a polycationic block is now arranged directly after the anchor block.

The conversion of TMA was determined from ^{1}H NMR samples of the quenched reaction mixture. Since oxygen was removed prior to polymerization by purging with argon, which was ascertained to also remove some Sty, the respective fraction of this monomer was calculated from the purified polymers by comparing the aromatic signals with signals of TMA. All polymers were treated with ca. 6 M hydrochloric acid at 115 °C overnight to hydrolyze the phosphonic acid ester. 1,4-Dioxane was added as cosolvent in case of AP4 and AP5 in order to obtain clear solutions. This is remarkable for the latter since it has a comparably low fraction of the hydrophobic monomer with Sty/TMA = 0.26. This suggests that the TMA-Sty-block structure has a more significant effect on the overall behavior of the polymer chain in solution compared to a mixed composition. This also reflects in the severe deviation of the average molar masses of this polymer derived from NMR spectroscopy and SEC (24000 g mol^{-1} (NMR) versus 40000 g mol^{-1} (SEC)) since the analytical methods focused on different polymer features – end groups (NMR) versus hydrodynamic volume assessment (SEC). Further SEC provides an apparent molar mass that relies on the SEC reference used, the conformation of the chain, and on its aggregation state.

Although there is no sign of degradation observed in ^{1}H NMR spectra, after hydrolysis the dispersities of each polymer increase by 0.1–0.2 which may be attributed to the harsh reaction conditions. The treatment with TMSBr was not possible for these polymers since no suitable solvent was found that was compatible with the reactant and able to dissolve the polymer.[7] The complete removal of methoxy groups was confirmed by the characteristic shift from 31.8 to 19.3 ppm in ^{31}P NMR spectra and the absence of the respective signals in ^{1}H NMR spectra.

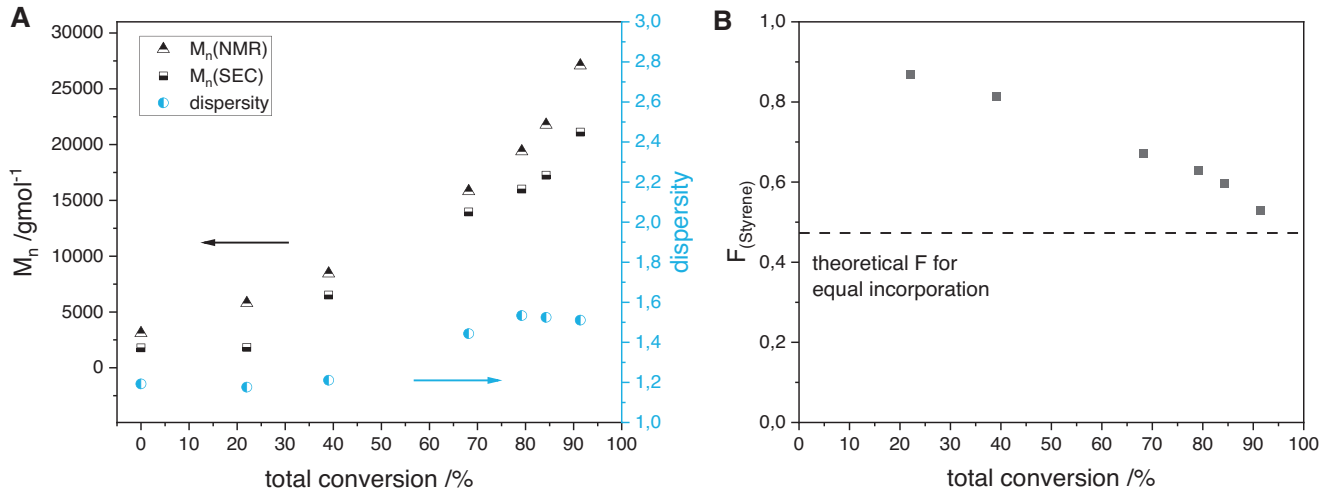

Figure 2. A) Evolution of molar mass derived from NMR spectroscopy and SEC as well as dispersity over total conversion for kinetics of P(DMVBP-b-Sty-grad-TMA). B) Fraction of Sty F_{Sty} over total conversion.

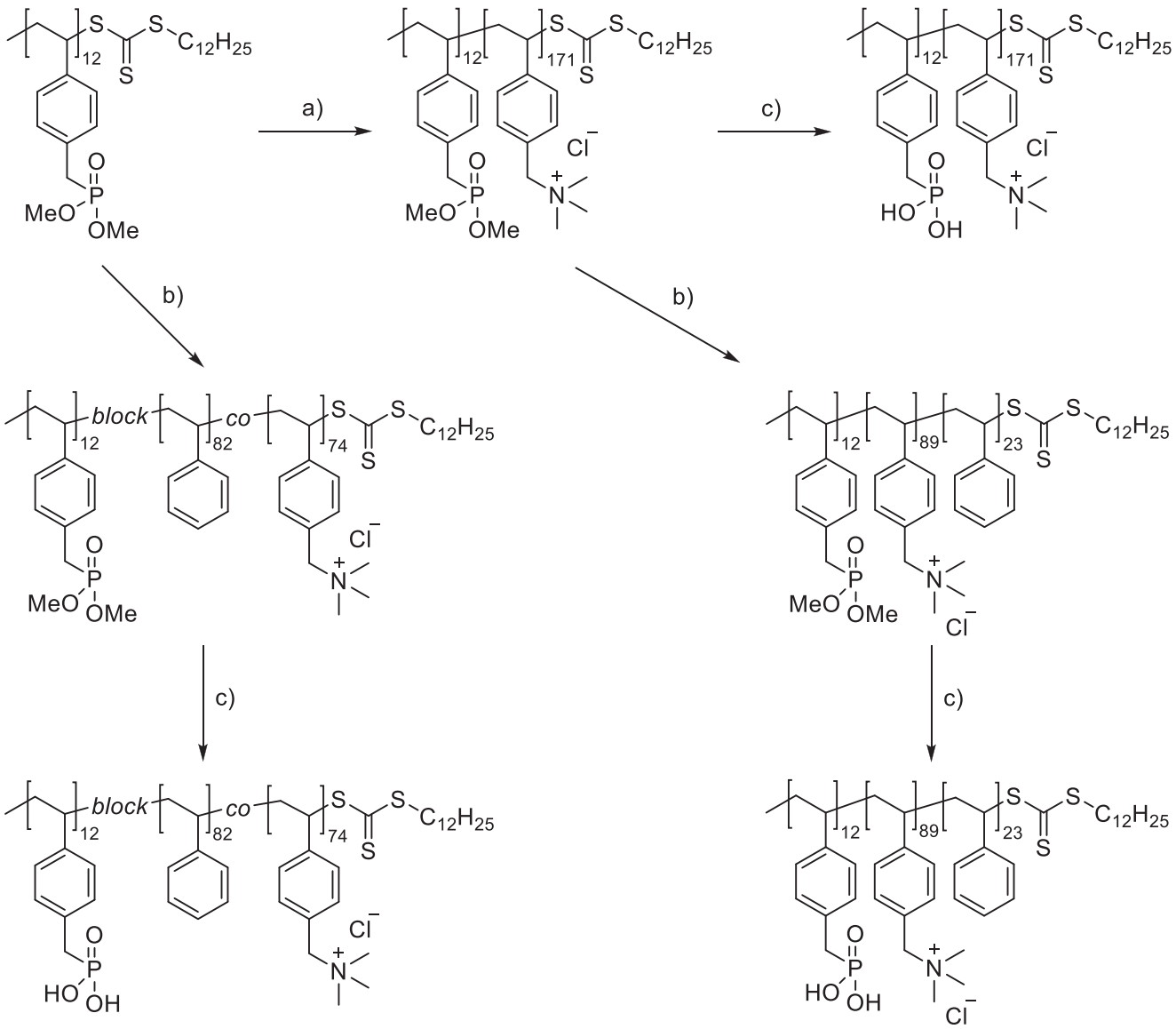

Figure 3. Exemplary reaction scheme for the synthesis of different AP. Reaction conditions: a) TMA, AIBN, dry DMF, 70 °C, 23 h; b) Sty/TMA or Sty, respectively, AIBN, DMF/H_2O, 70 °C, 20–24 h; c) conc. HCl/H2O 1:1, reflux, 23 h.

Table 1. Polymers with different fractions of Sty synthesized by block extension of P(DMVBP$_{12}$) in DMF/H_2O mixtures at 70 °C with AIBN as initiator and subsequent hydrolysis of DMVBP-units with HCl in water or water/1,4-dioxane.

Polymer		M_n (NMR) /g mol^{-1}	M_n (SEC) /g mol^{-1}	*D*	Sty/TMA	TMA units/mmol g^{-1}
AP1	P(VBPA$_{12}$-b-TMA$_{171}$)	39000	46000	1.62	0	4.38
AP2	P(VBPA$_{12}$-b-Sty$_{14}$-co-TMA$_{111}$)	28000	38000	1.55	0.13	3.96
AP3	P(VBPA$_{12}$-b-Sty$_{82}$-co-TMA$_{74}$)	27000	32000	1.55	1.11	2.74
AP4	P(VBPA$_{12}$-b-Sty$_{47}$-co-TMA$_{23}$)	13000	16000	1.53	2.04	1.77
AP5	P(VBPA$_{12}$-b-TMA$_{89}$-b-Sty$_{23}$)	24000	40000	1.64	0.26	3.71

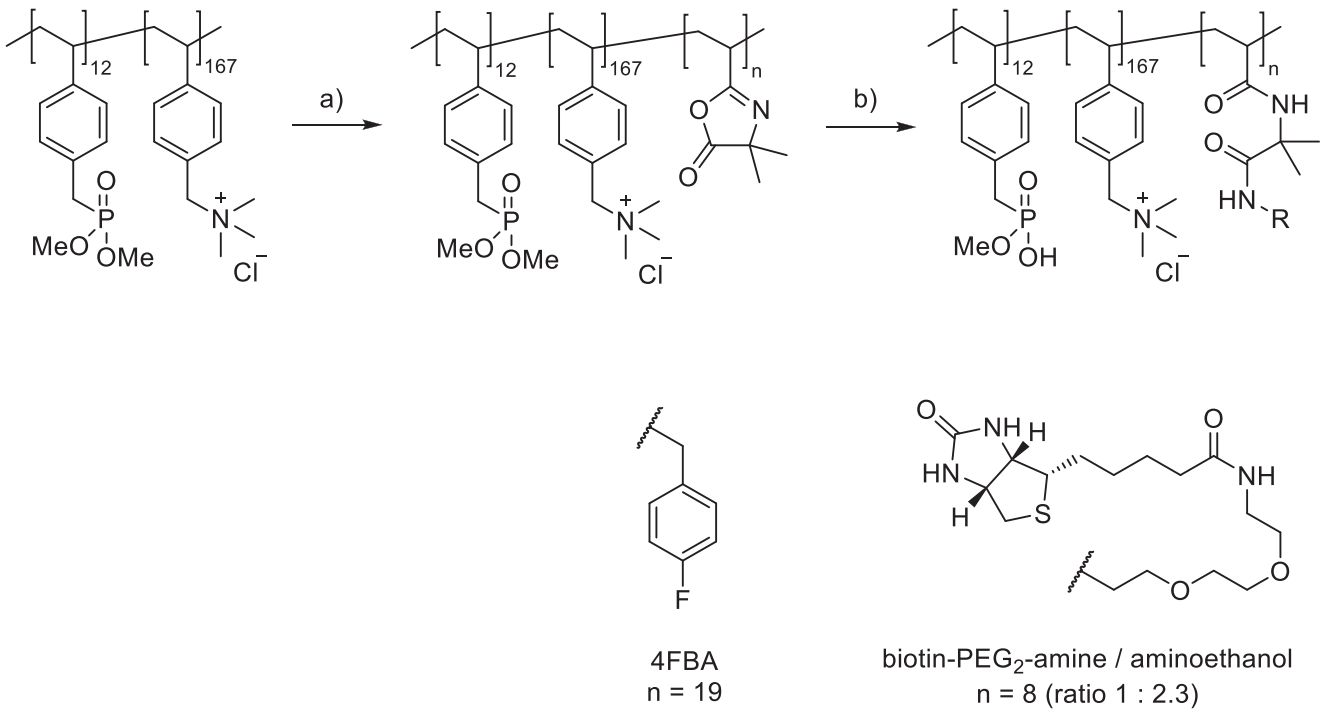

Figure 4. Exemplary reaction scheme of block extension with VDMA and subsequent ring-opening with 4FBA and biotin-PEG_2-amine, respectively. n denotes the degree of polymerization of VDMA and the quantity of functionalized units with the particular biomolecules, respectively. Reaction conditions: a) VDMA, AIBN, dry DMSO, 70 °C, 5 h; b) 4FBA or Biotin-PEG2-amine, room temperature, 17 h, then quenching of residual VDMA with aminoethanol.

The results demonstrate that the system Sty/TMA is suitable for the use as amphiphilic antimicrobial block: it allows the chain extension of the anchor block with both cationic and hydrophobic moieties simultaneously. Thus, the overall amphiphilic balance can be tuned by varying the monomer feed.

2.2. End Functionalization for Analysis of Immobilized Polymers

To be able to introduce further functionalities into the block copolymers, synthetic access to an end functionalization of the polymer was targeted. As one example for a suitable terminus biotin-poly(ethylenglycol)diamine (biotin-PEG_2-amine) was used to generate a biotin end functionalization. This molecule is frequently used for biochemical labeling or recognition due to its specific and strong affinity to certain proteins.[16–18] This is potentially beneficial for surface analytics of the applied polymer brush. Among others, prior works of Kuckling et al. have demonstrated the use of 2-vinyl-4,4-dimethylazlactone (VDMA) as a monomer in RAFT polymerizations in order to introduce an electrophilic moiety that selectively reacts with nucleophiles in a click-like manner (Figure S1, Supporting Information).[19,20] Here, the base polymer composed of anchor block and the antimicrobial block is to be chain extended with a small quantity of VDMA and subsequently modified with biotin sequence.

Since the fraction of end-attached groups was kept low, it was obvious that the analysis and verification of the obtained structure would be challenging. In order to prove both the block extension of the macro-RAFT agent and the incorporation of the chosen nucleophile, a model system was investigated at first using a fluorinated nucleophile as probe. P(DMVPA_{12}-b-Sty$_{39}$-co-TMA_{64}) was chain extended with VDMA in dry dimethylsulfoxide (DMSO) and AIBN as initiator at 70 °C for 5 h (**Figure 4**; Figure S1, Supporting Information). The reaction mixture was quenched and a conversion of 38% was determined via ^{1}H NMR spectroscopy by comparing the integral of methyl groups of free and polymerized VDMA. 4-Fluorobenzylamine (4FBA) was added as ring-opening agent and the polymer was isolated via dialysis and lyophilization. The comparison of SEC traces of precursor and product reveal a uniform shift to higher molar mass which verified the block extension. The emergence of a broad peak at 24.8 ppm next to the dimethyl phosphonate signal at 29.2 ppm (traces of HCl were added to protonate the acidic groups) in the ^{31}P NMR spectrum revealed that the phosphonate groups were partly dealkylated. It has been reported that the reaction of phosphonate esters with nucleophilic amines selectively yields the onefold dealkylated monoester.[21,22] A broad resonance in the ^{19}F NMR spectrum at −116.8 ppm proved the incorporation of the fluorinated compound and the absence of low-molecular residual nucleophile (Figure S2, Supporting Information). Upon addition of 4FBA to the NMR sample, its sharp resonances were observed next to the broad peak caused by the fluorine containing polymer. In the ^{1}H NMR spectrum, broad superimposing peaks of the aromatic protons at 6.8–7.5 ppm and the benzylic methylene group at 4.0–4.5 ppm could be assigned to polymer-bound 4FBA. This experiment validates the overall

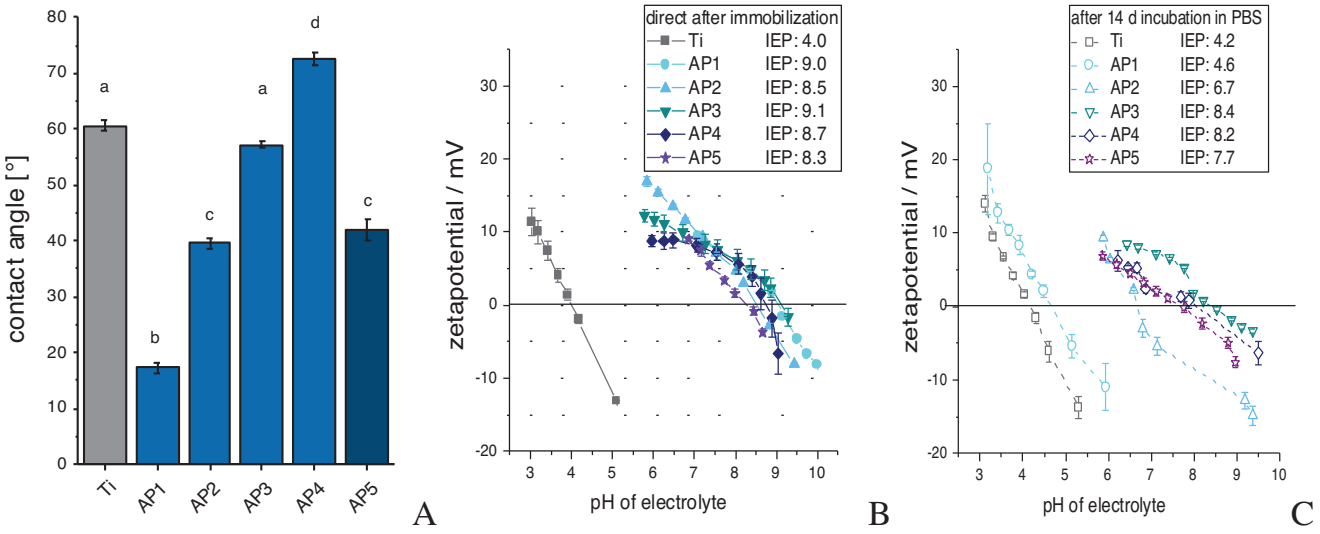

Figure 5. Physicochemical characterization: A) Water contact angle measurements using the sessile drop method, B) Zetapotential measurements by means of streaming potential for pairs of two oppositely arranged samples direct after immobilization and C) after 14 d of incubation.

concept by proving both that the macro-RAFT agent can readily be chain extended with VDMA and also reacts with the chosen nucleophile.

Next, biotin-PEG2-amine was used to generate a biotin end functionalization. P(DMVBP$_{12}$-b-TMA$_{167}$) was used as precursor and reacted with VDMA and AIBN as initiator in dry DMSO at 70 °C (Figure 4). The ^{1}H NMR spectrum of the quenched samples revealed a conversion of ≈30% yielding a block with just under ten VDMA-units in both cases.

After the polymerization was quenched, 0.3 equivalents of biotin-PEG$_2$-amine with respect to the total amount of azlactone-units in the mixture were added to obtain the biotin-functionalized polymer. Comparing ^{1}H NMR spectra before and after addition, a new set of vinyl protons was observed (Figure S3, Supporting Information). Depending on the integrals used for calculation, 25% to 33% of VDMA units underwent the ring-opening reaction, which is in good agreement with the equivalents added and amounts to ≈2.4 biotin-units per chain, assuming equal reactivity of free and polymer-bound azlactone. The remaining heterocycles were quenched by the addition of excess aminoethanol, after which the polymer was isolated by dialysis and lyophilization. The analysis via SEC confirmed the chain extension as the elution volume peak shifted from 17.60 to 17.41 mL corresponding to an increase in average molar mass from 40000 to 41000 g mol^{-1} (PMMA calibration). The dispersity was raised from 1.44 to 1.58, indicating presumably an irregular consumption of polymer-bound azlactone groups by the nucleophile. In the ^{31}P NMR spectrum, a single broad peak at 18.6 ppm was observed which indicated that the phosphonate was quantitatively mono-dealkylated to yield the monoester. Due to this dealkylation this polymer is regarded as suitable for further adsorption studies as well. Based on this characterization the polymer is abbreviated as P(MMVBP$_{12}$-b-TMA$_{167}$-b-PBio$_2$).

2.3. Functionalization of Titanium Surfaces and Their Physicochemical Characterization

As a next step the polymers varying in amphiphilic balance as well as final location of cationic versus hydrophobic monomer units (AP1 to AP5 as defined in Table 1) were used to prepare coatings on top of titanium samples (polished commercially pure Ti disks). The coatings were first characterized with respect to the physicochemical properties and then subjected to biological tests (see chapter 2.4). First, it was of interest whether the tuned amphiphilic balance could influence the wetting behavior of the respective coatings. Indeed, the water contact angle increased from 17.3 ± 0.9° to 72.5 ± 1.1° (**Figure 5**A) in correlation with the increasing Sty/TMA ratio of the polymers used (Table 1). The two polymers with a relatively similar ratio – AP2 with 0.26 and AP5 of 0.13 – yielded comparable contact angles of ≈40°, indicating that the order of TMA and Sty has no influence on the wetting behavior of the immobilized polymers. The first two polymers of this series were able to decrease the contact angle compared to the titanium reference and to form rather hydrophilic coatings, while AP4 (polymer with the highest Sty/TMA ratio) resulted in a significantly higher contact angle than the reference.

Zetapotential measurements demonstrate a remarkable positive shift in the isoelectric point (IEP) of the coated surfaces versus uncoated titanium reference by more than 5 pH units (Figure 5B) in a rather similar manner for all five tested polymers. This is much higher than for previous synthesized antimicrobial polymers based on quaternized vinylpyridinium polymers and reveals the presence of a very high content as well as good accessibility of positively charged components.[7] Only the triblock polymer with the reversed block order (AP5) revealed a somewhat less positive shift, but still the positive charges are seemingly well accessible. For all studied polymers this results in a slight positive charge at physiological pH compared to the negative charge

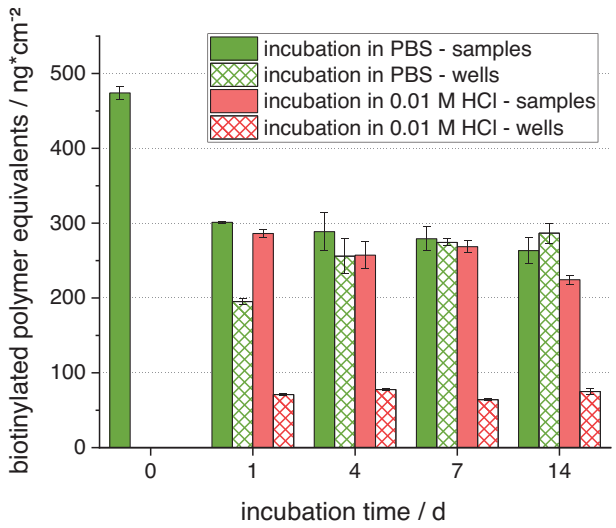

Figure 6. Stability of the coating with biotinylated polymer P(MMVBP12-b-TMA167-b-PBio$_2$), incubated for up to 14 d either in 37 °C in PBS or 0.01 M HCl.

of polished neutral titanium reference, which is based on preferential adsorption of hydroxyl ions.[23]

If the samples were stored for 14 d under nearly physiological conditions in phosphate-buffered saline (PBS) at pH 7.4 and 37 °C, more obvious differences occurred (Figure 5C). Now the order of shift in IEP corresponds quite well with the hydrophobicity – the higher the relative Sty content the more positive charges were retained on the surface, as long as the general structure is similar (AP1-AP4). Highest decrease of initially positive charge was observed for AP1 with the longest polycationic chain and without any Sty. It can be assumed that the more hydrophobic polymers result in higher stability due to additional hydrophobic interaction toward hydrophobic patches on titanium surfaces (always present on dried titanium surfaces)[7] or between hydrophobic parts of neighboring adsorbed polymers.

A semiquantitative analysis of one immobilized polymer type as well as its stability was performed for the biotinylated polymer P(MMVBP12-b-TMA167-b-PBio$_2$) (Figure 4). It is nearly comparable in its composition to AP1 and was immobilized using the same protocol as for the other tested polymers.

The semi-quantitative estimation is comparable to an enzymatic immunoassay but skipping the antibody-based steps. Here, the quantification of the immobilized biotinylated molecules is directly based on the high-affinity binding between biotin and streptavidin. Streptavidin with the coupled enzyme horseradish peroxidase (HRP) is bound in a first step in a concentration-dependent manner according to the amount of the immobilized polymer. Then, in a second step the detection is based on the development of a yellow-colored product that is enzymatically cleaved from the detection reagent. This method gives a semi-quantitative estimation, thus allowing for a relative comparison of the stability of the polymer-coated samples under different treatment options. When the samples with adsorbed polymer were incubated for 24 h, a decrease in the remaining coating density was observed, while further storage for up to 14 d resulted in only a minimal further reduction (**Figure 6**). This is consistent with the detection of biotinylated polymer in the well plates used for incubation, which show a slowly increasing amount of polymer desorbed from samples and then accumulated at the well surface (see bars with green pattern in Figure 6). When the coated samples were incubated in 0.01 M HCl (pH 2.0), a slightly greater reduction in the remaining polymer was observed than for incubation in PBS. However, in the case of incubation in HCl, the adsorption of the polymer on the surface of the wells was significantly lower, which might be explained due to a low adsorption onto the plastic surface at this pH. Both effects (influence of incubation time and incubation medium) were comparably small but statistically significant when analyzed using a two-way anova ($p < 0.05$).

Since the end-functionalization of the polymers with biotin is rather tedious, another method for semi-quantitative analysis (staining with the anionic dye Bengal rose already used to quantify biguanide coatings) was selected.[24] After incubation of coated samples for 24 h a violet staining of coated samples was visible that corresponded to the loss of optical density (OD) at 549 nm (**Figure 7A**). Calibration gives a nearly linear dependence between 1 and 10 µg mL^{-1} with nearly similar reaction, irrespective of whether the polymers are dissolved in water or dried onto titanium samples (Figure S4, Supporting Information). Unexpectedly, the extent of staining is only partially dependent on TMA content per total mass of polymer (compare last column in Table 1, varying between 1.77 and 4.38 mmol TMA units per g) as nearly all polymer types result in similar calibration curves. Only the most hydrophobic polymer AP4 with a distinguishably lower TMA content shows a markedly different slope (Figure S4, Supporting Information). The loss of absorbance lies in the nonlinear region above 10 µg for the more hydrophobic polymers AP3 and AP4, while AP2 and AP5 with comparatively low Sty content show a comparatively low extent of bound dye (corresponding to 0.5 – 1 µg polymer per sample) even directly after immobilization. AP1 featuring a long TMA chain can initially be immobilized to an intermediate density but shows a tremendous change when incubated for 14 d in PBS, consistent with the zetapotential data (Figure 5C), where for this polymer the greatest change in IEP after incubation was observed. This demonstrates that the higher the hydrophobicity the better the stability of adsorbed polymers under physiological conditions.

All the results of the physico-chemical analyses are reflected in the schematic model (Figure 7B), which shows the assumed state of initial adsorption and after rearrangements associated with partial desorption. The chain ends with the phosphonate anchor group as part of each AP (blue circles in Figure 7B) favor oriented adsorption due to its high affinity to titanium (oxide) surfaces. The strongest changes between initial situation and after incubation were observed for AP1, which can be explained by rearrangements due to the strong repulsive forces. AP2 and AP5 with a low percentage of hydrophobic Sty, but long polycationic segments, start with a lower initial density. Here, the molecules might form micelle-like structures before adsorption, which leads to a lower accessibility of the phosphonate anchor in the adsorption step. After adsorption, however, the interaction of the hydrophobic patches ensures increased stability against desorption. For AP5, it is assumed that the interaction of the two hydrophobic ends leads to lower chain flexibility in the adsorbed state. AP3 and AP4 with a Sty content of more than 50% are able

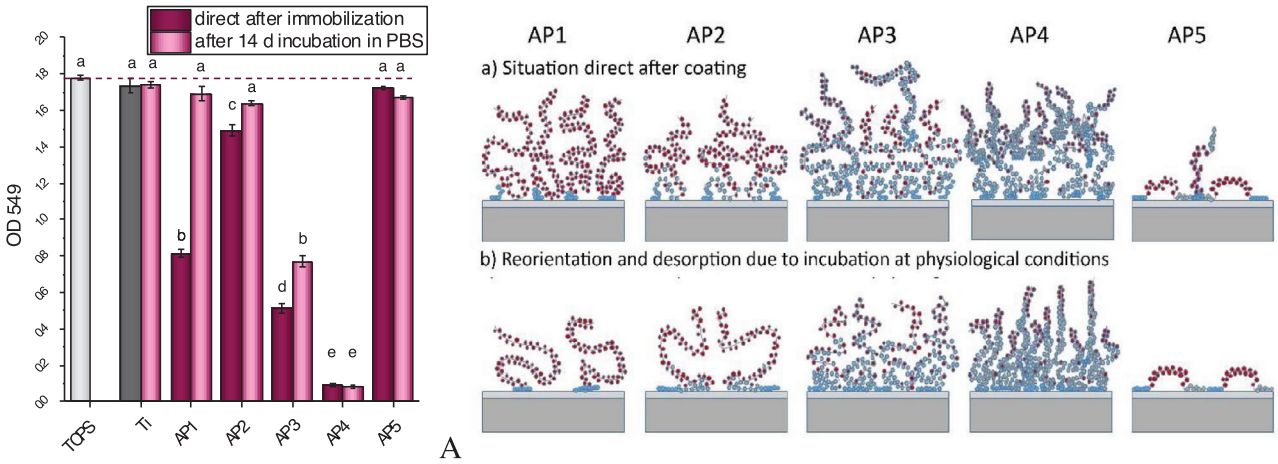

Figure 7. A) Bengal rose staining directly after coating process and after 14 d of incubation in PBS at 37 °C, B) resulting schematic model of immobilized polymers prior and after prolonged storage under physiological conditions.

to form a continuous film in the adsorbed state, which is even visible to the eye. In both cases, hydrophobic interactions with both the titanium (oxide) surface and the neighboring polymers are expected, resulting in high stability against desorption.

2.4. Biological Characterization of Functionalized Titanium Surfaces

The coated samples were exposed to solutions containing bacteria, either for a comparatively short time of 2 h under nutrient-rich conditions or for 17 h under nutrient-poor conditions, which favor the formation of a biofilm. In nutrient-rich conditions there was a clearly reduced number of bacteria attached to all polymer coated samples compared to the uncoated reference. However, each coating resulted in slightly different outcomes. While bacteria on AP1 (aside from phosphonate block with solely TMA units) and AP5 (polymer with triblock structure) were nearly all vital (nearly exclusive green color in Live/Dead staining with only a few dead bacteria comparable to the control staining in **Figure** 8A) the percentage of dead cells was higher on polymers with increasing hydrophobicity. While on AP2 (Sty/TMA ratio = 0.13) nearly half of attached bacteria were killed, on AP3 with the further increased hydrophobicity (Sty/TMA ratio = 1.11) nearly all of the few attached bacteria were dead. In contrast, for AP4 with the overall highest Sty/TMA ratio of 2.04 almost no bacteria were found at all, while the homogeneous green color results from a thick autofluorescent polymer film on top of the samples. This is consistent with the quantification of viable detachable bacteria after this period (as seen in Figure S5A, Supporting Information). When the samples were incubated with a nutrient-poor medium, biofilm formation was possible on all sample types with only a slight reduction of the number of vital bacteria attached on all polymer coated samples (Figures S5 and S6B, Supporting Information). However, one specific property of the polymer coated samples has to be highlighted: When the samples were treated with a comparatively gentle detachment procedure, almost complete detachment was observed on all sample types with TMA as the outer part of the polymer chain (AP1-AP4), while a high proportion of vital bacteria still remained on the samples in AP5 with the triblock structure and reversed TMA-Sty order and on the titanium reference (Figure 8B).

This reflects the superior cleanability of all coatings where the hydrophilic TMA block tends to be concentrated at the end of the polymer away from the surface (see schematic representation in Figure 8B), with no significant differences in terms of absolute polymer size and Sty/TMA ratio.

The lower adhesion of the bacteria under nutrient-rich conditions might be attributed to a slight anti-adhesive effect of all positively charged surfaces in combination with the hydration of the flexible hydrophilic chain ends. On the other hand, an additional killing effect is observed with an increase in hydrophobicity from only slight biocidal effect for the polymer consisting purely of TMA (AP1) to almost complete (for those few attached) at balanced ratios between the total Sty/TMA ratio as well as with the excess of Sty (AP3 and AP4). This is in agreement with many publications that show the bactericidal effect when combining positive charges and hydrophobic molecular components.[6,8]

Interestingly, in a layer-by-layer approach, it was postulated that the nanoscale surface heterogeneity of hydrophobic and positively charged patches could be the controlling factor for reduced protein adsorption and thus improved antifouling properties.[25] This might explain the strongly reduced bacterial adhesion on all mixed polymers, due to an intrinsic heterogeneity of the two non-uniformly distributed monomer units.

Our findings of increased antimicrobial effect with increased hydrophobicity are also in line with findings from Oda et al., who varied percentage and distribution of hydrophobic components.[15] However, it has to be emphasized that their experiments were performed with soluble polymers while our polymers are fixed to surfaces promoting an orientation of phosphonate anchor and adjacent hydrophobic parts toward the surface and hydrophilic charged parts rather oriented toward the surrounding solution. The intramolecular aggregation due to hydrophobic parts and the potential inactivity seen in Oda et al. are therefore not as detrimental in our case, as they potentially stabilize the interaction with the surface.[15] In the middle part we assume a mixed composition resulting in chains of sufficient flex-

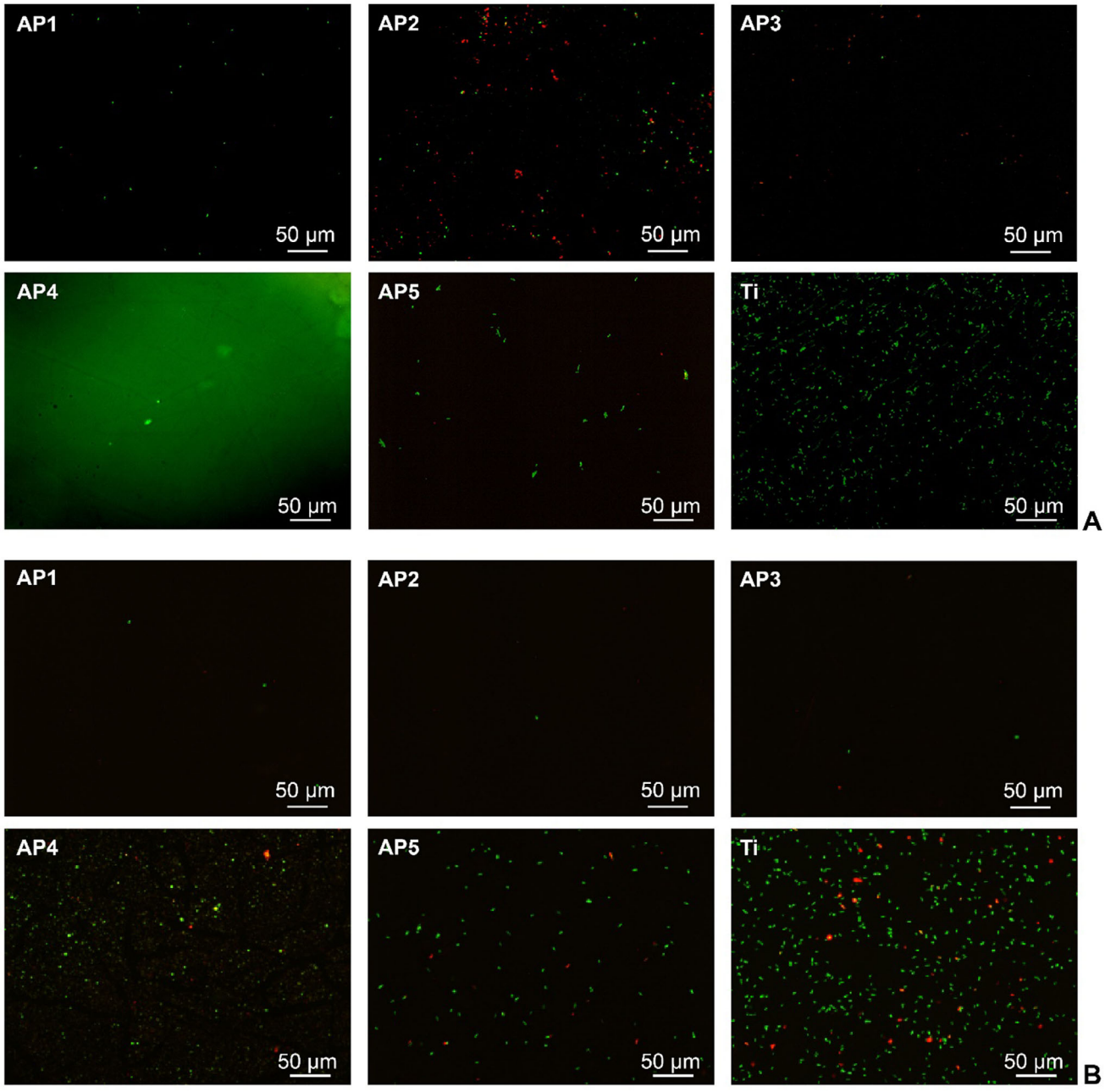

Figure 8. Live/dead staining of bacteria at functionalized surfaces for either: A) short adhesion of 2 h in high nutrient conditions in LB medium (after washing) or B) for 17 h growth of biofilm in low nutrient condition, here after gentle detachment (30 s vortex, 30 s ultrasonic bath, 30 s vortex).

ibility followed by exclusively positively charged final parts oriented toward the solution, building the basis for a certain antiadhesive effect as well as interactions with bacterial membranes. Similar reductions for using only hydrophilic cationic polymers based on poly[2-methacryloyloxyethyl] trimethyl-ammonium chloride were already observed by Dinghra et al. but for a grafting from approach.[26] In our "grafting-to" approach, we work with pre-synthesized polymers, and in addition to the increase of desired antimicrobial effect, the graft density as well as the stability of the coatings were also positively influenced by increasing hydrophobicity of the polymers.

In contrast, we believe that the triblock polymer with the Sty block positioned at the end of the molecule could adopt a fixed arrangement where both the anchor and the hydrophobic block interact strongly with the surface, thus diminishing the mobility of the positively charged block in the center of the polymer. However, this flexibility seems to be a crucial requirement particularly for biocidal effects but also for antiadhesive efficacy in early adhesion and for cleanability of later formed biofilms.

The overall reduced antimicrobial effect observed under nutrient-poor conditions might be explained by transition to biofilm mode. By addition of glucose as a simple carbon

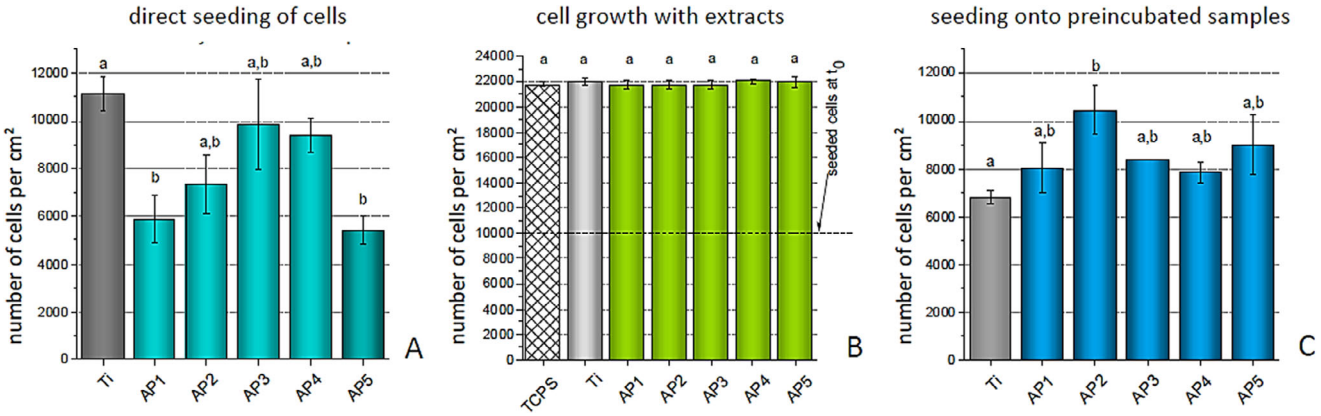

Figure 9. Cytotoxicity of coated samples to human gingival fibroblasts: A) Direct adhesion of gingival fibroblast on top of coated titanium samples, B) Growth of gingival fibroblasts seeded in cell culture polystyrene wells cultured with extracts of differently coated titanium samples incubated for 24 h in cell culture medium, C) Adhesion of cells seeded on such pre-incubated samples.

source it was shown that *E. coli* strains tend to produce strong biofilms compared to planktonic state in nutrient-rich condition in lysogeny broth (LB) medium.[27] Under such conditions the bacteria are generally less susceptible to antimicrobial attacks and the excreted extracellular polymeric substances (EPS) might shield the bacterial membranes from the polymers. For our coatings the antiadhesive and biocidal effect is obviously not yet sufficient to prevent or minimize the bacterial adhesion for prolonged periods. In this respect, the positive charge could even have a counterproductive effect and attract negatively charged bacteria, as shown in van der Mey et al. for polydiallyldimethylammonium chloride (PDADMAC) coatings on glass.[28] However, even with other neutral brush coatings, the anti-adhesive effect was not high enough to completely prevent the adhesion of bacteria, but rather led to a delay in surface coverage.[29] Nevertheless, the superior cleaning ability of the coated samples should be emphasized once again, which enabled complete removal of these early biofilms formed under such starvation conditions. Here, too, the polymers with the flexible positively charged end (AP1-AP4) seem to be more effective than the triblock polymer, which we assume to take on a more rigid and fixed immobilization status. This phenomenon is also consistent with the easier removal of bacteria by applied shear stress observed for other hydrophilic brushes.[29] However, it has to be verified in further long-term experiments if also matured biofilms can be easily removed from such coated surfaces.

Finally, the AP3 with balanced Sty/TMA composition and a sufficiently long positive cluster in a flexible, non-bonded chain would prove to be a good candidate to reduce initial adhesion, provoke biocidal activity under nutrient-rich conditions as well as good cleanability to remove formed biofilms and that also has a stable bonding to the titanium surface for the intended use under physiological conditions.

When antimicrobial surfaces are introduced into the body, cytocompatibility must of course be guaranteed. For dental implants and abutments, cytocompatibility with gingival fibroblasts is of great interest. When such cells were seeded directly onto the functionalized samples, a slight but non-significant reduction in adhesion was observed for all surfaces with TMA block at the end compared to the polished references, especially for the most hydrophilic coatings, while the one polymer coating with the Sty block at the end (AP5) resulted in a significantly lower cell adhesion (**Figure 9A**). To determine whether this effect was due to anti-adhesive properties or cytotoxic effects, cytocompatibility was also indirectly investigated by means of extract analysis. For this purpose, the functionalized samples were incubated in cell medium and after 24 h of incubation, this medium was used for further cell cultivation of cells pre-cultured in different well plates. All cells were able to grow in the same way for both positive controls and all types of extracts (Figure 9B), and cell morphology was not at all affected in this indirect assay (Figure S7, Supporting Information). When the cells were seeded onto the 24 h pre-incubated samples, all cells were able to adhere to a similar extent as the controls, and the cell morphology on the samples was also excellent, showing well-spread cells on all functionalized samples (**Figure 10**). This demonstrates improved cytocompatibility than for the previously synthesized polymers, where cell morphology was strongly affected.[7] Particularly for abutments surfaces, which are in close contact to the gum tissues of the periodontal pockets no adverse effects of such coatings would be expected and even cell adhesion would not be hampered.

2.5. Further Coating Developments

In order to develop coatings with even longer persistence against desorption or degradation, the question arose whether a polymer molecule, which is regio-selectively anchored via the phosphonate anchor block, could be partially embedded into anodically thickened titanium oxide layers. The idea behind this is illustrated in **Figure 11A**.

During anodic polarization, the thickness of the native titanium oxide layer at the two phase boundaries oxide/electrolyte and oxide/metal increases to almost the same extent, as Ti^{4+} and O_2^- migrate simultaneously toward the electrolyte and metal, respectively. This growth mechanism leads to a two-layer system in which electrolytic species such as ions and previously adsorbed molecules can be incorporated into the outer part of the oxide layer grown at the oxide/electrolyte interface. Under the current conditions, an effective formation potential of 4 V was applied,

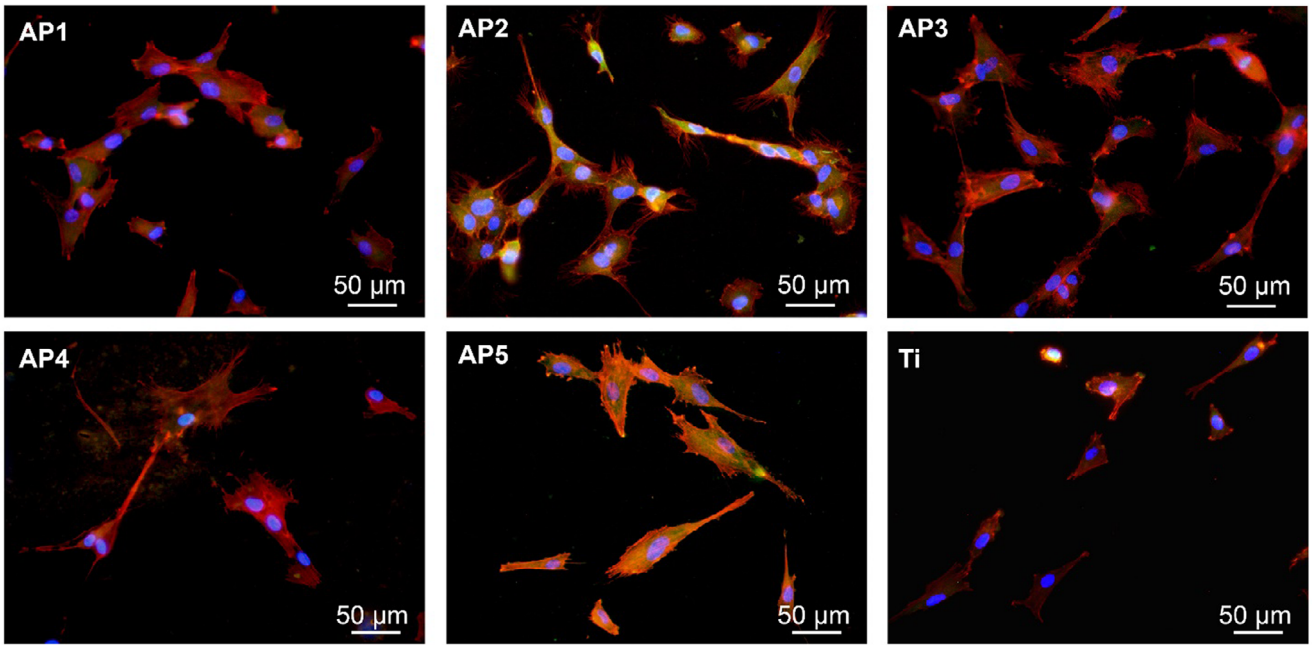

Figure 10. Adhesion of human gingival fibroblasts on pre- incubated samples stained for cell nuclei (blue), actin cytoskeleton (red) and vinculin (green) – belonging to condition shown in Figure 9C.

which corresponds to an oxide growth of ≈4 nm of the outer oxide layer. The underlying mechanism and possible side effects are described in more detail in Beutner et al.[30]

First promising results were obtained for the longest polymer with 171 TMA units. Anodization directly after the heat curing step with or without intermediate washing steps as well as anodization in presence of freshly added polymer in the electrolyte resulted in a clear presence of positive charges reflected by an isoelectric point (IEP) higher than 8.0 for all conditions (Figure 11B). When such samples with anodically fixed polymer AP1 were incubated for 14 d in PBS, a certain reduction of positive charge was observed, but still an IEP of ≈6.0 was obtained compared to the IEP of 4.6 observed for the purely adsorbed AP1 after the same incubation period (Figure 5C).

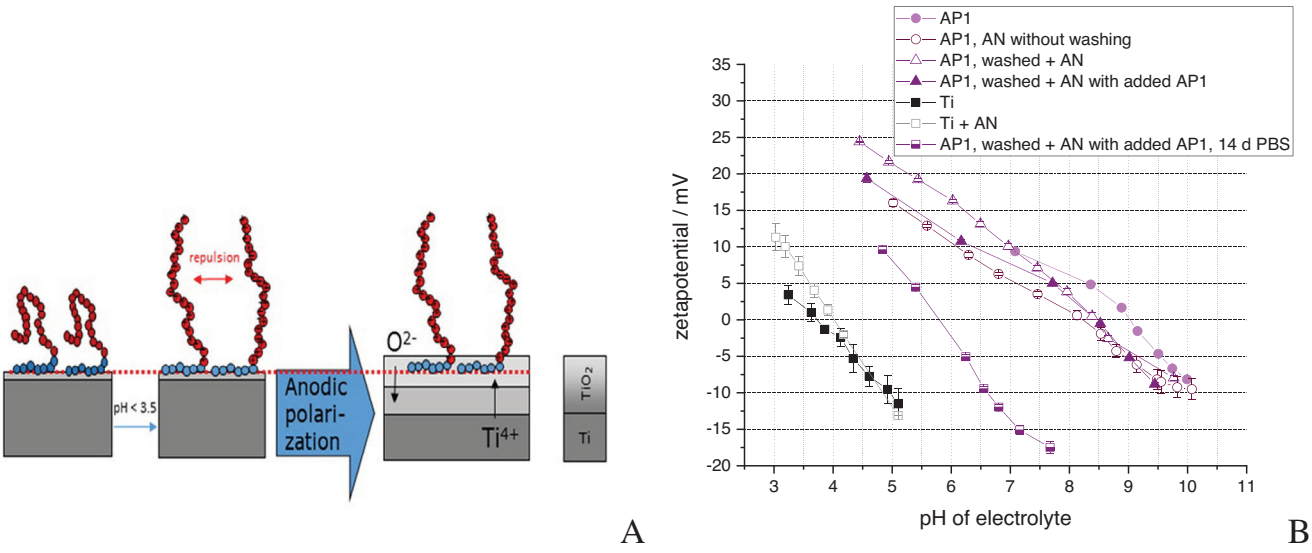

Figure 11. Partial integration of antimicrobial polymers via anodical thickening of native oxide layer: A) schematic illustration of the process – polymers with phosphonate anchor interact with native titanium oxide layer, in acidic environment the steric repulsion between different polymer chains as well to positively charged substrate surface provokes an elongated polymer orientation, anodic oxidation leads to oxide thickening toward bulk material as well into the electrolyte thereby embedding initially adsorbed polymers, B) verification of positive charge of immobilized polymers for the starting situation of heat cured adsorbed AP1 as well as after anodic oxidation (AN) for three different protocol types.

This is consistent with the stability measurements for the anodically fixed biotinylated polymer, which showed a slightly lower initial amount of polymer equivalents but a higher persistence of the immobilized coating upon incubation in PBS (Figure S8, Supporting Information).

3. Conclusion

In order to adjust the compatibility of adsorbable antimicrobial polymers with human cells versus their antimicrobial activity, the block composition of a polycationic segment was modified regarding the amphiphilic balance. Hereto, the combination of the hydrophobic monomer Sty and the cationic monomer TMA was explored. The kinetics of the copolymerization using the anchor segment precursor P(DMVBP$_{12}$) as macro-RAFT agent were investigated and revealed that Sty was preferentially incorporated, leading to a slight gradient in monomer sequence. Overall, the reaction exhibited the characteristics of a controlled polymerization and demonstrated that the system is suitable for the intended use. Thus, a series of polymers with varied ratios of Sty to TMA in the second block were synthesized and post modified to liberate the phosphonic acid groups of the anchor block. They can be used in biological evaluation to gain insight into the optimal composition of amphiphilic polymer brushes made by "grafting to".

With P(DMVBP$_{12}$-b-TMA$_{167}$) as precursor, another strategy to improve biocompatibility was pursued: the diblock copolymer was chain extended with VDMA to introduce a short segment of terminal electrophilic groups that could be modified in a "click"-like manner. Preliminary experiments with a fluorine-containing probe demonstrated that both the block extension and the ring-opening reaction worked as intended. Next, biotin-PEG$_2$-amine was used as nucleophile to obtain a polymer that can be investigated in biochemical assays by taking advantage of specific protein-biotin-interactions.

The modified block composition fundamentally changed the behavior of titanium samples coated with such newly synthesized polymers, resulting in significantly improved cytocompatibility. The antimicrobial activity could also be tuned by the Sty/TMA ratio. However, the contact-killing properties of such coatings might be masked for longer incubation in nutrient-poor conditions promoting biofilm formation, nonetheless even under such nutrient-poor conditions a reduced initial bacterial adhesion was seen and particularly a remarkable cleanability that allows for almost completely removal of adherent biofilms with only gentle treatment. However, a flexible, positively charged outer part seems to be the prerequisite for this effect, while triblock polymers with positively charged block fixed in the middle of the polymer are not efficient for the purpose of immobilizing polymers on biomaterial surfaces.

4. Experimental Section

Materials: 4-Vinylbenzyl chloride (90%) and styrene (Sty) were purchased from Merck and distilled before use. AIBN (98%) was purchased from Merck and recrystallized from ethanol before use. 2-(Dodecylthiocarbonothioylthio)-2-methylpropionic acid (DMP, 98%), 4-fluorobenzylamine (97%), and LB medium were purchased from Merck and used as received. Dulbecco's Modified Eagle Medium (DMEM), 10% fetal bovine serum, glutamate, penicillin, and streptomycin were purchased from Merck Biochrom. Human gingival fibroblasts were purchased from CellBiologics, Chicago, IL. Trimethylamine (4.2 M in EtOH) and Biotin-PEG$_2$-Amine (95+%) were purchased from Fluka and TCI, respectively. DMF (extra dry over molecular sieves) and 1,4 dioxane (99.5%) were purchased from Thermo Scientific. Ethanol (99.5%), DMSO (99), and acetonitrile (99.5%) were purchased from Grüssing.

Methods: NMR spectra were recorded on a Bruker Avance 500 and a Bruker Ascent 700 and processed using Bruker TopSpin. The chemical shifts (δ) were listed in ppm and coupling constants (J) were listed in Hz, respectively. The monomer conversion was determined from ^{1}H NMR samples of the quenched reaction mixture by comparing integrals of monomer and polymer signals.

Dialysis was performed with Spectra Pore 6 dialysis membranes (MWCO = 1 kD) against water or as specified in the procedure. An Alpha 2–4 LDplus freeze dryer by Christ was used to remove water afterward.

Attenuated total reflection infrared (IR) spectra were recorded on the Bruker "Vertex 70" spectrometer and processed using ACD/spectrus.

The samples were analyzed by means of electrospray ionization mass spectrometry (ESI-MS) using a "Synapt-G2 HDMS" mass spectrometer from "Waters" with a time-of-flight analyzer.

UV/vis spectra were recorded on an Analytik Jena Specord 50 PLUS UV/vis spectrophotometer using Aspect UV software.

Size exclusion chromatography (SEC) was performed with HFIP + 0.05 M CF_3COOK as eluent in a system with two consecutive columns (PSS-PFG, 10^3 and 10^2 Å) and a Merck L-6200 pump operating at 1 mL min^{-1}. A Shodex RI 101 detector was employed to obtain the molar masses and dispersities according to a PMMA standard. A second system with THF as eluent and two consecutive columns (PPS-SDV 10^5 and 10^3 Å) and a Merck L-6200 pump operating at 1 mL min^{-1} with a Knauer RI detector was employed. The system was calibrated using polystyrene standards.

Monomers—Synthesis of 2-Vinyl-4,4-dimethylazlactone (VDMA): VDMA was synthesized according the literature.[31]

Monomers—Synthesis of 4-vinylbenzyltrimethyl Ammonium Chloride (TMA): 4-vinylbenzyl chloride (12 mL, 85.2 mmol) was dissolved in ethanol (20 mL) and cooled to 0 °C. Within 20 min, trimethylamine in ethanol (4.2 M, 24.3 mL, 10 mmol) was added. The reaction was allowed to come to room temperature and stirred for 19 h. Ethanol and residual trimethylamine were removed in vacuo. The raw product was recrystallized from acetonitrile to yield TMA (10.27 g, 45.5 mmol, 57%) as colorless crystals.

^{1}H NMR (DMSO-*d6*, 700 MHz) δ (ppm): 3.05 (s, 9H, C**H**$_3$), 4.54 (s, 2H, Ar-C**H**$_2$), 5.36 (dd, 1H, $^2J_{HH}$ = 0.8 Hz, $^3J_{HH}$ = 10.7 Hz, CH = C**H**$_{trans}$), 5.96 (dd, 1H, $^2J_{HH}$ = 0.8 Hz, $^3J_{HH}$ = 17.7 Hz, CH = C**H**$_{cis}$), 6.80 (dd, 1H, ^{3}JHH = 10.9 Hz, $^3J_{HH}$ = 17.7 Hz, C**H**), 7.51 (dd, 2H, Ar-**H**), 7.61 (dd, 2H, Ar-**H**)

^{13}C NMR (176 MHz, DMSO-*d6*) δ (ppm): 52.1 (**C**H$_3$), 67.7 (Ar-**C**H$_2$), 116.2 (CH-**C**H$_2$), 126.5 (**C**$_{Ar}$-H), 127.8 (**C**$_{Ar}$), 133.1 (**C**$_{Ar}$-H), 135.8 (Ar-**C**H), 138.9 (**C**$_{Ar}$)

ESI-ToF-MS: calculated: 176.1434 g mol^{-1} [M-Cl$^-$]$^+$, found: 176.1424 g mol^{-1}

T_m = 260 °C (decomposition)

Polymers—Synthesis of P(DMVBP$_{12}$): P(DMVBP) was synthesized according the literature.[7]

Polymers—Synthesis of P(DMVBP$_{12}$-b-TMA$_{171}$): In a typical reaction, P(DMVBP$_{12}$) (87.9, 0.02 mmol), TMA (1198.6 mg, 5.66 mmol), and AIBN (0.9 mg, 5 µmol) were dissolved in DMF (5 mL) and water (5 mL) in a Schlenk tube with a rubber Septum and a stirring bar. The solution was purged with argon for 20 min and placed in a preheated oil bath at 70 °C afterward. After stirring for 23 h, the reaction was quenched by freezing the mixture with liquid nitrogen and exposure to air. For the determination of monomer conversion, a sample was taken and examined by ^{1}H NMR spectroscopy. The polymer was isolated by dialysis and lyophilization as a colorless solid (94% conversion, 732.4 mg, 57% yield).

Polymers of the general structure P(DMVBP-b-TMA) could also be isolated by precipitation from isopropanol.

^{1}H NMR (D_2O, 500 MHz) δ (ppm): 0.63-0.87 (br, $C_{11}H_{22}$-C**H**$_3$), 1.05-2.30 (br, C**H**$_2$-C**H** and C_{10}**H**$_{20}$), 2.74-3.24 (br, N-C**H**$_3$), 3.51-3.85 (br, P-OC**H**$_3$), 4.16-4.66 (br, N-C**H**$_2$-Ar and P-C**H**$_2$-Ar), 6.34-7.61 (br, P-CH$_2$-Ar**H** and N-CH$_2$Ar**H**)

^{31}P NMR (DMSO-*d6*, 202 MHz) δ (ppm): 31.3-32.2 (br, P)

$M_{n(theo., NMR)}$ = 30000 g mol^{-1}

SEC (HFIP + 0.05 M CF_3COOK, calibration with PMMA): M_n = 40000 g mol^{-1}, D = 1.44

Polymers—Synthesis of P(VBPA$_{12}$-b-TMA$_{171}$): In a typical reaction, P(DMVBP$_{12}$-b-TMA$_{171}$) (7 g, 0.28 mmol) were dissolved in water (40 mL) and conc. HCl (40 mL). The mixture was heated to 115 °C for 23 h, whereby the solution became increasingly turbid. Afterward, the polymer was isolated via dialysis and lyophilization to yield a colorless solid (4.4698 g, 0.18 mmol, 64%).

^{1}H NMR (D_2O, 500 MHz) δ (ppm): 0.93-0.98 (br, $C_{11}H_{22}$-C**H**$_3$), 1.21-2.30 (br, C**H**$_2$-C**H** and C_{10}**H**$_{20}$), 2.70-3.27 (br, N-C**H**$_3$), 4.23-4.64 (br, N-C**H**$_2$-Ar and P-C**H**$_2$-Ar), 6.42-7.49 (br, P-CH$_2$-Ar**H** and N-CH$_2$Ar**H**)

^{31}P NMR (DMSO-*d6*, 202 MHz) δ (ppm): 18.3-21.4 (br, P)

$M_{n(theo., NMR)}$ = 39000 g mol^{-1}

SEC (HFIP + 0.05 M CF_3COOK, calibration with PMMA): M_n = 46000 g mol^{-1}, D = 1.62

Polymers—Synthesis of P(DMVBP$_{12}$-b-TMA$_{89}$-b-Sty$_{23}$): P(DMVBP$_{12}$-b-TMA$_{89}$) (486.0 mg, 0.02 mmol), Sty (218.7 mg, 2.10 mmol) and AIBN (0.9 mg, 5 µmol) were dissolved in DMF (4.5 mL) and water (3 mL) in a Schlenk tube with a rubber Septum and a stirring bar. The solution was purged with argon for 30 min and placed in a preheated oil bath at 70 °C afterward. After stirring for 20 h, the reaction was quenched by freezing the mixture with liquid nitrogen and exposure to air. The polymer was isolated by dialysis and lyophilization as a light-yellow solid (conversion not determinable, 390.2 mg, 0016 mmol, 72% yield).

The degree of polymerization of Sty was determined from the ^{1}H NMR spectrum of P(DMVBP$_{12}$-b-TMA$_{89}$-b-Sty$_{23}$) by comparing signals from TMA with the aromatic signals.

^{1}H NMR (D_2O, 500 MHz) δ (ppm): 1.07-2.26 (br, C**H**$_2$-C**H** and C_{10}**H**$_{20}$), 2.65-3.20 (br, N-C**H**$_3$), 3.50-3.75 (br, P-OC**H**$_3$), 4.15-4.56 (br, N-C**H**$_2$-Ar and P-C**H**$_2$-Ar), 6.20-7.59 (br, Ar**H**$_{Sty}$, P-CH$_2$-Ar**H** and N-CH$_2$Ar**H**)

^{31}P NMR (DMSO-*d6*, 202 MHz) δ (ppm): 31.2-32.4 (br, P)

$M_{n(theo., NMR)}$ = 24300 g mol^{-1}

SEC (HFIP + 0.05 M CF_3COOK, calibration with PMMA): M_n = 30000 g mol^{-1}, D = 1.45

Polymers—Synthesis of P(VBPA$_{12}$-b-TMA$_{89}$-b-Sty$_{23}$): P(DMVBP$_{12}$-b-TMA$_{89}$-b-Sty$_{23}$) (360.0 mg, 0.018 mmol) was dissolved in water (1.5 mL), 1,4-dioxane (3 mL) and conc. HCl (1.5 mL). The solution was heated to reflux for 18 h and isolated by dialysis and lyophilization. The product was obtained as a colorless solid (348.9 mg, 0.015 mmol, 81%).

^{1}H NMR (D_2O, 500 MHz) δ (ppm): 0.85-2.25 (br, C**H**$_2$-C**H** and C_{10}**H**$_{20}$), 2.55-3.39 (br, N-C**H**$_3$), 4.06-4.64 (br, N-C**H**$_2$-Ar and P-C**H**$_2$-Ar), 6.27-7.70 (br, P-CH$_2$-Ar**H** and N-CH$_2$Ar**H**)

^{31}P NMR (DMSO-*d6*, 202 MHz) δ (ppm): 18.4-20.4 (br, P)

$M_{n(theo., NMR)}$ = 24000 g mol^{-1}

SEC (HFIP + 0.05 M CF_3COOK, calibration with PMMA): M_n = 40000 g mol^{-1}, D = 1.65

Polymers—Synthesis of P(DMVBP$_{12}$-b-Sty$_{82}$-co-TMA$_{74}$): In a typical reaction, P(DMVBP$_{12}$) (103.3 mg, 0.03 mmol), TMA (707.4 mg, 3.34 mmol), Sty (349.4 mg, 3.35 mmol), and AIBN (1.1 mg, 7 µmol) were dissolved in DMF (6 mL) and water (4 mL) in a Schlenk tube with a rubber Septum and a stirring bar. The solution was purged with argon for 30 min and placed in a preheated oil bath at 70 °C afterward. After stirring for 24 h, the reaction was quenched by freezing the mixture with liquid nitrogen and exposure to air. The polymer was isolated by dialysis and lyophilization as a light-yellow solid (TMA conversion 81%, 722.3 mg, 62% yield).

The degree of polymerization of Sty was determined from the ^{1}H NMR spectrum of P(VBPA$_{12}$-b-TMA$_{89}$-b-Sty$_{23}$) by comparing signals from TMA with the aromatic signals.

^{1}H NMR (D_2O, 500 MHz) δ (ppm): 0.60-2.26 (br, C**H**$_2$-C**H** and C_{10}**H**$_{20}$), 2.59-3.22 (br, N-C**H**$_3$), 3.47-3.83 (br, P-OC**H**$_3$), 4.04-4.67 (br, N-C**H**$_2$-Ar and P-C**H**$_2$-Ar), 5.98-7.83 (br, Ar**H**$_{Sty}$, P-CH$_2$-Ar**H** and N-CH$_2$Ar**H**)

^{31}P NMR (D_2O, 202 MHz) δ (ppm): 30.6-32.4 (br, P)

$M_{n(theo., NMR)}$ = 27000 g mol^{-1}

SEC (HFIP + 0.05 M CF_3COOK, calibration with PMMA): M_n = 26000 g mol^{-1}, D = 1.34

Polymers—Synthesis of P(VBPA$_{12}$-b-Sty$_{82}$-co-TMA$_{74}$): In a typical reaction, P(DMVBP$_{12}$-b-Sty$_{82}$-co-TMA$_{74}$) (700.0 mg, 0.03 mmol) was dissolved in water (2.5 mL) and conc. HCl (2.5 mL) and heated to reflux for 23 h. The polymer was isolated by dialysis and lyophilization to obtain the product as a light-yellow solid (631.5 mg, 0.023 mmol, 78%).

^{1}H NMR (D_2O, 500 MHz) δ (ppm): 0.92-0.99 (br, $C_{11}H_{22}$-C**H**$_3$), 1.04-2.35 (br, C**H**$_2$-C**H** and C_{10}**H**$_{20}$), 2.61-3.24 (br, N-C**H**$_3$), 4.14-4.64 (br, N-C**H**$_2$-Ar and P-C**H**$_2$-Ar), 6.20-7.73 (br, Ar**H**$_{Sty}$, P-CH$_2$-Ar**H** and N-CH$_2$Ar**H**)

^{31}P NMR (D_2O, 202 MHz) δ (ppm): 18.4-20.9 (br, P)

$M_{n(theo., NMR)}$ = 27000 g mol^{-1}

SEC (HFIP + 0.05 M CF_3COOK, calibration with PMMA): M_n = 32000 g mol^{-1}, D = 1.55

Polymers—Synthesis of P(DMVBP$_{12}$-b-Sty$_{39}$-co-TMA$_{64}$-b-4FBA$_{19}$): P(DMVBP$_{12}$-b-Sty$_{39}$-co-TMA$_{64}$) (89.7 mg, 4.3 µmol), VDMA (32.0 mg, 0,23 mmol) and AIBN (0.1 mg, 0.6 µmol) were dissolved in dry DMSO (2 mL) in a Schlenk tube with a rubber septum and a stirring bar. The solution was purged with argon for 30 min and placed in a preheated oil bath at 70 °C afterward. After stirring for 5 h, the reaction was quenched by freezing the mixture with liquid nitrogen and short exposure to air. For the determination of monomer conversion, a sample was taken and examined by ^{1}H NMR spectroscopy (38% VDMA conversion). Then, 4-fluorobenzylamine (27 µL, 0.24 µmol) was added and the solution was stirred overnight. The product (94 mg, 3.6 µmol, 84%) was isolated as a colorless solid by dialysis and lyophilization.

^{1}H NMR (DMSO-*d6*, 700 MHz) δ (ppm): 0.80-0.89 (br, $C_{11}H_{22}$-C**H**$_3$), 0.92-2.30 (br, C**H**$_2$-C**H** and C_{10}**H**$_{20}$), 2.76-3.30 (br, N-C**H**$_3$), 3.45-3.66 (br, P-OC**H**$_3$), 3.91-4.42 (br, NH-C**H**$_2$), 4.41-5.18 (br, N-C**H**$_2$-Ar and P-C**H**$_2$-Ar), 6.07-7.58 (br, Ar**H**$_{Sty}$, P-CH$_2$-Ar**H** and N-CH$_2$Ar**H**), 7.89-8.59 (br, N**H**)

^{19}F NMR (DMSO-*d6*, 659 MHz) δ (ppm): -117.6-(-115.9) (br, F)

^{31}P NMR (DMSO-*d6*, 202 MHz) δ (ppm): 24.4-25.0 (br, P(OH)(OCH$_3$)), 28.8-29.5 (br, P-(OCH$_3$)$_2$)

$M_{n(theo., NMR)}$ = 26000 g mol^{-1}

SEC (HFIP + 0.05 M CF_3COOK, calibration with PMMA): M_n = 21000 g mol^{-1}, D = 1.74

IR (ATR, $\tilde{\nu}$, cm^1, selected bands): 1489 (s, C—H) 1645 (vs, C═C), 2924 (m, C—H), 3026 (w, C-H$_{Ar}$)

Polymers—Synthesis of P(DMVBP$_{12}$-b-TMA$_{167}$-b-Biotin$_2$): P(DMVBP$_{12}$-b-TMA$_{167}$) (500.6 mg, 12.8 µmol), VDMA (57 mg, 0.41 mmol) and AIBN (1.0 mg, 6 µmol) were dissolved in dry DMSO (9.8 mL) in a Schlenk tube with a rubber septum and a stirring bar. The solution was purged with argon for 20 min and placed in a preheated oil bath at 70 °C afterward. After stirring for 5 h, the reaction was quenched by freezing the mixture with liquid nitrogen and short exposure to air. For the determination of monomer conversion, a sample was taken and examined by ^{1}H NMR spectroscopy (32% VDMA conversion). Then, biotin-PEG$_2$-amine (46 mg, 0.12 mmol, 0.3 equivalents with respect to VDMA) was added and the solution was stirred for 17 h. A ^{1}H NMR sample was taken and ethanolamine (410 µL, 6.6 mmol) was added to quench residual azlactone groups. After stirring for 7 h and storage in the fridge for 3 d, the polymer was isolated by dialysis and lyophilization and obtained as colorless solid (444.5 mg, 10.8 µmol, 85%).

^{1}H NMR (DMSO-*d6*, 500 MHz) δ (ppm): 0.86-2.26 (br, C**H**$_2$-C**H**), 2.67-3.19 (br, N-C**H**$_3$), 3.47-3.69 (br, P-OC**H**$_3$), 4.13-4.79 (br, N-C**H**$_2$-Ar and P-C**H**$_2$-Ar), 6.11-7.56 (br, P-CH$_2$-Ar**H** and N-CH$_2$-Ar**H**)

^{31}P NMR (DMSO-*d6*, 202 MHz) δ (ppm): 18.0-19.0 (br, P)

$M_{n(theo., NMR)}$ = 41000 g mol^{-1}

SEC (HFIP + 0.05 M CF_3COOK, calibration with PMMA): M_n = 41000 g mol^{-1}, D = 1.58

IR (ATR, $\tilde{\nu}$, cm^1, selected bands): 1385 (m, C—H) 1427 (m, C—H) 1485 (s, C—H) 1645 (s, C═C) 2923 (w, C-H) 3022 (w, C-H$_{Ar}$)

Titanium References and Polymer-Coated Samples: Flat discs of commercially pure titanium grade 2 with sample sizes of 10 mm diameter and 2 mm height were first cutted from commercially pure titanium rods grade 2 (cpTi) of 10 mm diameter with 0.02 m min^{-1} feed rate at 80 rpm, resulting in comparably smooth "machined" samples, which were cleaned by

ultrasonic baths of acetone, and ultrapure water. Afterwards the samples were fixed in self-created Teflon holders and vibration polished for 17 h using a commercially available fleece cloth and MasterMet 2 Suspension (Buehler). Afterward the samples were washed twice in sterile ultrapure water and dried in a laminar flow box prior to use.

Coating of samples was performed with 1 mM of each polymer dissolved in methanol (p.a.) covering the complete surface for 2 h in a small, closed container saturated with methanol vapor. Subsequently, 100 µL of water was added and incubated for another 60 min and then the solution was removed. Heat curing was performed for 17 h at 120 °C. Afterwards samples were washed under vigorous shaking with 1 mL of phosphate-buffered saline (PBS), followed by two rinsing steps with 1 mL of ultrapure water, each for 5 min. The samples were then air-dried in a laminar flow bench and stored under sterile conditions for subsequent analyses. Reference samples were treated identically with the adsorption step performed with pure methanol.

Streaming Potential Measurements: Measurements of zetapotential were performed by means of a commercial electrokinetic analyzer (EKA, Anton Paar GmbH, Austria) equipped with a gap cell. For each experiment a set of two discs was mounted via double-sided tape onto sample holders resulting in a parallel orientation and the channel was adjusted to ≈150 µm.

The electrolyte consisted of 0.001 M KOH, which was automatically titrated with 0.1 M HCl or 0.1 M KOH in a pH range of 3.0 – 9.0, depending on initial potential. Pressure profiles were recorded from 0 to 250 mbar and four measurement points per titration step were analyzed. The zetapotential values were calculated from determined streaming potential according to the Fairbrother-Mastin method by means of software supplied by the manufacturer.

Bacterial Experiments: All experiments were performed with a model strain of a genetically modified *E. coli* K12 (SM2029) that had a green fluorescent protein (GFP) marker, resistance to kanamycin and was modified for biofilm formation in minimal medium kindly provided by Dr. Boschke, TU Dresden.[32,33]

Analysis of Attachment under nutrient-rich conditions: Onto coated samples lying in a 48 well plate (for suspension culture, Nunc) 50 µL of a bacterial solution containing 10^8 colony forming units (CFU) mL^{-1} was dropped, while all outer wells and spaces between wells were filled with sterile water to generate an atmosphere saturated with water vapor. After 2 h incubation time samples were washed 3 times with PBS for 5 min and then prepared for live/dead staining as described below.

Analysis of Attachment and Biofilm Formation under starving conditions: in modified M9 minimal medium simply called biofilm medium (BF). The receipt for this medium and the bacteria adhesion experiment can be found in Kaiser et al.[34] In brief, coated titanium samples and respective uncoated reference samples, all disinfected with UV irradiation for 30 min, were seeded by placing 100 µL of a bacteria suspension containing 10^8 CFU mL^{-1} onto the surfaces for 1 h at 30 °C. After this, the bacteria suspension was removed and immediately rinsed 3 times with 100 µL PBS. Cultivation of samples with remaining attached bacteria was continued under dynamic conditions for 17 h at 30 °C hanging in reverse position in 24 well plates filled with 1.2 mL BF medium per well. The fraction of bacteria being only weakly attached was removed by three washing steps with 1.2 mL PBS under shaking for 5 min. Subsequently, the attached bacteria were completely removed by three consecutive steps of vortexing, ultrasonic bath, and repeated vortexing (30 s each) with the samples placed in 50 mL Falcon tubes filled with 1 mL of LB medium. The number of viable bacteria was determined by means of a proliferation assay described in detail Kaiser et al.[34]

Live/Dead Staining: Staining of the samples was performed with the live/dead kit (Invitrogen) according to the manufacturer's instructions, followed by the three rinsing steps with PBS prior or after the detachment steps. Staining of individual samples was conducted immediately prior to fluorescence microscopy. Pictures were taken with a cLSM 510 meta (Zeiss, Jena, Germany).

Biocompatibility Assessment: Primary human gingival fibroblasts (Cellsystems, Germany) were used in 6th passage and cultivated in Dulbecco's Modified Eagle Medium (DMEM) supplemented with 10% fetal bovine serum, 2 mM glutamate, 100 U penicillin, and 100 µg ml^{-1} streptomycin (complete medium) in a humidified incubator with 5% CO_2.

Titanium samples coated with antimicrobial polymers as described above were disinfected by 30 min UV irradiation. Afterward they were transferred to 48 well plates (Nunclon Delta, Nunc) and cell seeding was performed by the addition of 1 mL cell suspension containing 10.000 cells either directly on coated samples or onto samples that were pre-incubated with 1 ml of complete cell culture medium for 24 h at 37 °C.

For indirect assessment of cytotoxicity cells were seeded into 24 well plates (TPP) with a density of 4000 cell cm^{-2}. After 24 h of initial attachment the medium was exchanged to the extracts obtained form 24 h incubation of each sample in 1 ml of complete medium and further cultivated for 48 h. Images of the cells in the wells were taken at the start and after 48 h of incubation with the extracts. Subsequently the cells were washed with PBS and then frozen at -80 °C until further analysis. All cells adherent either on tissue culture polystyrene wells (TCPS) or on samples were lysed on ice for 60 min in a lysis buffer consisting of 1% Triton X-100 in phosphate buffered saline. The number of cells was calculated based on the intracellular lactate dehydrogenase (LDH) activity released into the lysate with a commercially available LDH kit (TaKaRa Bio Inc.) according to the manufacturer's instructions and correlated with the cell number using a calibration curve.

After 24 h of cultivation, one sample per coating type was washed with PBS and fixed with 3.7% formaldehyde solution for 20 min at 4 °C. Prior to staining cells were permeabilized with 0.2% Triton X-100 in PBS for 2 min and then incubated first for 30 min in 1% bovine serum albumin (BSA, diluted in PBS). Afterward, samples were first incubated 1 h with antivinculin diluted 1:400 (Sigma) and in a 2nd step with 1 µg mL^{-1} of 4,6-Diamidino-2-phenyl-indol-dihydrochlorid, 2-(4-Amidinophenyl)-6-indolcarbamidin-dihydrochlorid (DAPI), AlexaFluor 546 Phalloidin (Invitrogen), diluted 1:50, and anti-mouse-IgG-Alexa488 (Life Technologies, diluted 1:2000 in 1% BSA in PBS. Samples were analyzed with a cLSM 510 meta (Zeiss, Germany) equipped with a charge-coupled device (CCD) camera.

Statistical Analysis: All experiments were carried out with $n = 4$ and results were shown as mean ± standard error. Bacterial and cell culture tests were performed in two independent experiments. Statistical analysis was performed using one-way or two-way Anova, with Tukey's post hoc test with respective correction for multiple comparisons of means. If Levene's test revealed no equal variances Sidak-Holm test was applied as post-hoc test. Significant differences were assumed at $p < 0.05$. Significant differences were assigned in the graphs for $p < 0.05$ by means of lower letters indicating no significant differences for all bars showing the same letter.

Supporting Information

Supporting Information is available from the Wiley Online Library or from the author.

Acknowledgements

C.W.B. and R.M. contributed equally to this work and shared first authorship. Open access funding enabled and organized by Projekt DEAL.

Conflict of Interest

The authors declare no conflict of interest.

Data Availability Statement

The data that support the findings of this study are available in the supplementary material of this article.

Keywords

antiadhesive surfaces, antimicrobial polymers, grafting to, polymer brushes

Received: February 18, 2025
Revised: March 24, 2025
Published online: April 10, 2025

[1] A. Trampuz, W. Zimmerli, *Injury* **2006**, *37*, 1822.
[2] D. G. Kennedy, A. M. O'Mahony, E. P. Culligan, C. M. O'Driscoll, K. B. Ryan, *Antibiotics* **2022**, *11*, 1822.
[3] D. Nathwani, G. Raman, K. Sulham, M. Gavaghan, V. Menon, *Antimicrob. Resist. Infect. Control* **2014**, *3*, 32.
[4] I. Babutan, A. D. Lucaci, I. Botiz, *Polymers* **2021**, *13*, 1552.
[5] L. Timofeeva, N. Kleshcheva, *Appl. Microbiol. Biotechnol.* **2011**, *89*, 475.
[6] Q. Song, S. Y. Chan, Z. Xiao, R. Zhao, Y. Zhang, X. Chen, T. Liu, Y. Yan, B. Zhang, F. Han, P. Li, *Prog. Org. Coatings* **2024**, *188*, 108214.
[7] R. Methling, O. Dückmann, F. Simon, C. Wolf-Brandstetter, D. Kuckling, *Macromol. Mater. Eng.* **2023**, *308*, 2200665.
[8] A. C. Engler, N. Wiradharma, Z. Y. Ong, D. J. Coady, J. L. Hedrick, Y. Y. Yang, *Nano Today* **2012**, *7*, 201.
[9] P. T. Phuong, S. Oliver, J. He, E. H. H. Wong, R. T. Mathers, C. Boyer, *Biomacromolecules* **2020**, *21*, 5241.
[10] P. Pham, S. Oliver, E. H. H. Wong, C. Boyer, *Polym. Chem.* **2021**, *12*, 5689.
[11] K. Suga, M. Murakami, S. Nakayama, K. Watanabe, S. Yamada, T. Tsuji, D. Nagao, *ACS Appl. Bio Mater.* **2022**, *5*, 2202.
[12] S. Kliewer, S. G. Wicha, A. Bröker, T. Naundorf, T. Catmadim, E. K. Oellingrath, M. Rohnke, W. R. Streit, C. Vollstedt, H. Kipphardt, W. Maison, *Colloids Surf., B: Biointerfaces* **2020**, *186*, 110679.
[13] Y. U. D. Semchikov, *Macromol. Symp.* **1996**, *111*, 317.
[14] E. V. Chernikova, S. D. Zaitsev, A. V. Plutalova, K. O. Mineeva, O. S. Zotova, D. V. Vishnevetsky, *RSC Adv.* **2018**, *8*, 14300.
[15] Y. Oda, S. Kanaoka, T. Sato, S. Aoshima, K. Kuroda, *Biomacromolecules* **2011**, *12*, 3581.
[16] D. Scharnweber, S. Bierbaum, C. Wolf-Brandstetter, *FEBS Lett.* **2018**, *592*, 2181.
[17] P. H. E. Hamming, J. Huskens, *ACS Appl. Mater. Interfaces* **2021**, *13*, 58114.
[18] W. L. Hurley, E. Finkelstein, B. D. Holst, *J. Immunol. Methods* **1985**, *85*, 195.
[19] J. Li, X. Yu, A. Herberg, D. Kuckling, *Macromol. Rapid Commun.* **2019**, *40*, 1800674.
[20] J. Li, C. Ji, X. Yu, M. Yin, D. Kuckling, *Macromol. Rapid Commun.* **2019**, *40*, 1900189.
[21] V. Vassileva, E. M. Georgiev, K. Troev, D. M. Roundhill, *Phosphorus Sulfur Silicon Relat. Elem.* **1994**, *92*, 101.
[22] D. E. Bryant, C. Kilner, T. P. Kee, *Inorg. Chim. Acta* **2009**, *362*, 614.
[23] R. Zimmermann, N. Rein, C. Werner, *Phys. Chem. Chem. Phys.* **2009**, *11*, 4360.
[24] P. Zwicker, N. Geist, E. Göbler, M. Kulke, T. Schmidt, M. Hornschuh, U. Lempke, C. Prinz, M. Delcea, A. Kramer, G. Müller, *Coatings* **2021**, *11*, 1118.
[25] S. Y. Wong, L. Han, K. Timachova, J. Veselinovic, M. N. Hyder, C. Ortiz, A. M. Klibanov, P. T. Hammond, *Biomacromolecules* **2012**, *13*, 719.
[26] S. Dhingra, S. Sharma, S. Saha, *ACS Appl. Bio Mater.* **2022**, *5*, 1364.
[27] J. Hu, X. Lv, X. Niu, F. Yu, J. Zuo, Y. Bao, H. Yin, C. Huang, S. Nawaz, W. Zhou, W. Jiang, Z. Chen, J. Tu, K. Qi, X. Han, *J. Appl. Microbiol.* **2022**, *132*, 4236.
[28] H. C. van der Mei, M. Rustema-Abbing, D. E. Langworthy, D. I. Collias, M. D. Mitchell, D. W. Bjorkquist, H. J. Busscher, *Biotechnol. Bioeng.* **2008**, *99*, 165.
[29] M. R. Nejadnik, H. C. van der Mei, W. Norde, H. J. Busscher, *Biomaterials* **2008**, *29*, 4117.
[30] R. Beutner, J. Michael, A. Förster, B. Schwenzer, D. Scharnweber, *Biomaterials* **2009**, *30*, 2774.
[31] M. E. Levere, H. T. Ho, S. Pascual, L. Fontaine, *Polym. Chem.* **2011**, *2*, 2878.
[32] A. Reisner, J. A. Haagensen, M. A. Schembri, E. L. Zechner, S. Molin, *Mol. Microbiol.* **2003**, *48*, 933.
[33] S. Mulansky, P. Goering, M. Ruhnow, F. Lenk, T. Bley, E. Boschke, *Heat Transfer Eng.* **2017**, *38*, 805.
[34] F. Kaiser, D. Scharnweber, S. Bierbaum, C. Wolf-Brandstetter, *Bioelectrochemistry* **2020**, *133*, 107485.

